Ultra-precision cutting on thin-walled cylinder with deformation estimation and compensation method

Kaiyang Xia[1], Yuanliu Chen[1#]

1 The State Key Lab of Fluid Power and Mechatronic Systems, Zhejiang University, 310027 Hangzhou, China
Corresponding Author / Email: yuanliuchen@zju.edu.cn, TEL: +86-0571-87952294, FAX: +86-0571-87952294

KEYWORDS: Thin-walled cylinder, Deformation estimation and compensation, Fast tool servo, Ultra-precision cutting

Thin-walled components have the characteristics of high strength and lightweight, so they are widely used in aviation, automobile and other industrial fields. However, the low stiffness of thin-walled workpieces causes them to be deformed by cutting forces during processing, which will seriously affect the surface morphology of the processed workpieces. To increase the processed surface dimensional accuracy, this paper proposed a deformation estimation and compensation method. Through finite element simulation, the axial deformation curve of the thin-walled cylinder was obtained, and experiments were carried out to verify it. Three capacitive displacement sensors are arranged on the same axis away from the cutting point. Based on the axial deformation curve, the deformation of the cutting point can be accurately estimated. The estimated deformation is then fed back to the fast tool servo, which can compensate for the deformation effectively. The cutting experiments were conducted, and a double sinusoidal microstructure was machined on the thin-walled cylindrical surface. The results showed that the circumferential morphology error and axial morphology error of the microstructure were highly reduced.

1. Introduction

In high-tech equipment, thin-walled structural parts can achieve lightweight products and improve operating efficiency while maintaining sufficient strength, which has become important components of equipment in aerospace, electronics and other fields [1]. Ultra-precision turning technology can provide high surface finishing quality, which is widely used in the processing of thin-walled structures. However, due to the inherent low stiffness characteristics of the thin-walled structure, the structure is prone to chatter and deformation during processing, resulting in poor surface roughness and high structural errors. The stability lobe diagram is often used to predict the cutting parameters in a chatter-free processing [2]. On the other hand, the deformation of the thin-walled structure induced by the cutting or clamping force is more intuitive, which will lead to undesired processing morphology, thereby affecting the service performance of the workpiece [3]. This paper will mainly focus on the deformation of thin-walled structures during the processing.

Since the geometric errors caused by deformation will inevitably occur during the machining of thin-walled components, many researchers have tried to monitor and estimate these deformations. The deformation can be estimated by finite elements models [4] and mechanistic models [5], which were derived from the experiments and theoretical analysis. After accurately estimating the deformation during the processing of thin-walled components, it is particularly important to perform deformation compensation [6]. Due to the advantages of high bandwidth and high positioning accuracy [7], fast tool servo (FTS) systems were used to compensate for the deformation induced by the clamping system [8].

To improve the processing accuracy and solve the deformation problem during processing, this paper presents a method for ultra-precision cutting on a thin-walled cylinder surface with FTS, which can estimate and compensate for the deformation at the processing point. The final cutting results shows that with the help of the deformation compensation method, the cutting accuracy has been significantly improved.

2. Principle and Experiment Setup

2.1 Principle of deformation estimation and compensation

Fig. 1 shows the principle of deformation estimation and compensation for the cylinder. The thin-walled cylinder is clamped on the spindle, the microstructure is machined by the voice coil motor actuated FTS (VCM-FTS). A deformation measurement system consisting of three displacement sensors is installed at the same level as the VCM-FTS. The position of these three sensors is presented as z_0, z_1 and z_2. The cylindrical part at position z_0 is solid, which means there is approximately no deformation induced. So, the sensor at z_0 is responsible for measuring the C-axis vibration. The other two sensors are used to measure the deformation of two points located on the same horizontal line as the processing point. Through the processing point deformation estimation algorithm, the deformation signal can be used to calculate the deformation of the processing point. The cutting trajectory can be generated by adding the ideal trajectory and the estimated deformation. With the servo controller, the VCM-

FTS produce deformation-compensated motion, which can effectively reduce the topography error of the thin-walled cylinder.

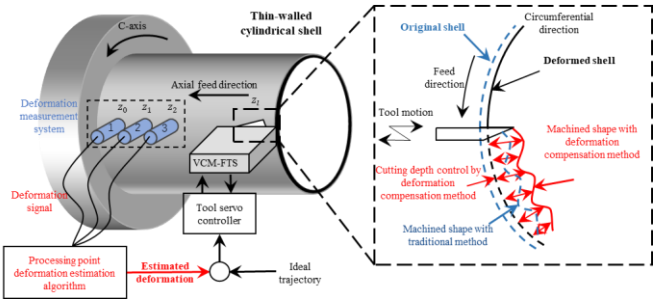

Fig. 1 Schematic diagram of real-time deformation compensation for the thin-walled cylinder at the cutting point.

For thin-walled cylinders of the same structure, which have the same radius, length and wall thickness, the deformation on the cylinder is only related to the external force exerted on it. The magnitude, frequency and force applied point will all affect the deformation of the thin-walled cylinder. The deformation u can be expressed as the following empirical formula,

$$u = k \cdot u^* = k \cdot f(z, l) \tag{1}$$

in which, k is a dimensionless force constant, which is proportional to the magnitude of the force. u^* represents the unit deformation, which corresponds to the deformation caused by an external force of 1 N. l represents the length from the fixed end to the force applied point. And z is the distance between the fixed point to the force applied point, namely, $z \in [0, l]$. The function f can be obtained by simulation, which will be introduced in section 3. The position of 3 displacement sensors and the processing point, are represented as z_0, z_1, z_2 and z_l. Therefore, the unit deformation of two sensors and the processing point, $u^*_{1,l}, u^*_{2,l}$ and $u^*_{l,l}$ can be expressed as Eq. (2-4).

$$u^*_{1,l} = f(z_1, l) \tag{2}$$

$$u^*_{2,l} = f(z_2, l) \tag{3}$$

$$u^*_{l,l} = f(z_l, l) \tag{4}$$

The force constant k can be calculated by the least squares fittin g method, which can be expressed as following equation,

$$k = \left(\begin{bmatrix} u^*_{1,l} & u^*_{2,l} \end{bmatrix} \begin{bmatrix} u^*_{1,l} \\ u^*_{2,l} \end{bmatrix} \right)^{-1} \left(\begin{bmatrix} u^*_{1,l} & u^*_{2,l} \end{bmatrix} \begin{bmatrix} u_{1,l} \\ u_{2,l} \end{bmatrix} \right) \tag{5}$$

in which, $u_{1,l}$ and $u_{2,l}$ is the actual deformation at point z_1 and z_2, which are obtained by the measurement system. After that, the actual deformation at processing point z_l can be obtained by multiplying force constant k and unit deformation $u^*_{l,l}$, as shown in Eq. (6).

$$u_{l,l} = k \cdot u^*_{l,l} \tag{6}$$

The process of deformation estimation and compensation algorithm is shown in Fig. 2. At the preprocessing step, the three displacement signals p_0, p_1 and p_2 are obtained by three sensors, at three points z_0, z_1 and z_2. Since the roundness of the workpiece at three points is different, to obtain the deformation, the roundness needs to be measured before processing, which is p^0_0, p^0_1 and p^0_2. Then the deformation value p'_0, p'_1 and p'_2, can be obtained as following equations,

$$p'_0 = p_0 - p^0_0 \tag{7}$$

$$p'_1 = p_1 - p^0_1 \tag{8}$$

$$p'_2 = p_2 - p^0_2 \tag{9}$$

In addition, to eliminate the disturbance caused by C-axis vibration, the actual deformation of thin-walled cylinder $u_{1,l}, u_{2,l}$ at two points z_1, z_2 can be obtained as follow,

$$u_{1,l} = p'_1 - p'_0 \tag{10}$$

$$u_{2,l} = p'_2 - p'_0 \tag{11}$$

Through the x-axis position signal obtained from the lathe, the force applied point l can be obtained. The unit deformation at points z_1, z_2 and z_l can be calculated with Eq. (1). Then by substituting both unit and actual deformation at z_1 and z_2 into Eq. (5), the force constant k can be obtained. Finally, the deformation at processing point $u_{l,l}$ can be calculated by Eq. (6). And then, it can be added into the ideal trajectory to realizing the deformation compensation.

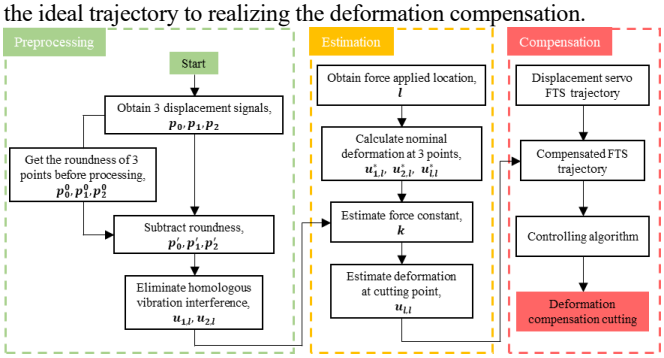

Fig. 2. Deformation estimation and compensation flow chart.

2.2 Structure and Control of VCM-FTS

The structure of the VCM-FTS is shown in Fig. 3(a). The VCM-FTS mainly consists of VCM, front and rear flexible hinges, and a capacitance displacement sensor. The VCM is used to drive the mechanical mechanism to produce reciprocating motion. The two flexible hinges can constrain the degree of freedom of the VCM to ensure that it can only move in one direction. Except for the hinge structure, the front flexible hinge also contains a lever structure, different end effectors can be equipped on it, which can avoid interference between the measurement system and the VCM-FTS during machining. The capacitive displacement sensor is used to measure the displacement of the end effector. The control block of VCM-FTS for thin-walled cylinder deformation compensation is shown in Fig. 3(b). $G(s)$ represents the transfer function of VCM-FTS system. The controller of VCM-FTS includes two parts, the basic part and the deformation estimation algorithm. The basic part also includes two parts, the damping controller $C_1(s)$ and the PI Controller $C_2(s)$, there transfer function are $C_1(s) = K_1 + K_2 s$ and $C_2(s) = K_p + K_i/s$, respectively.

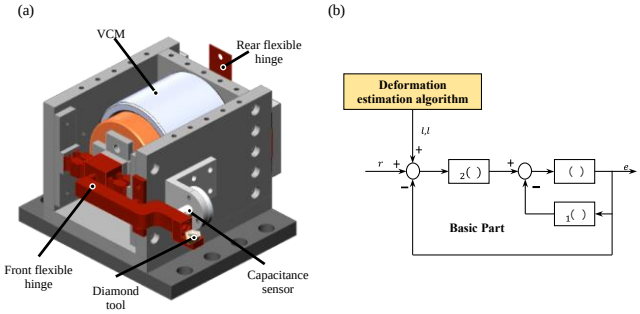

Fig. 3 (a) structure of VCM-FTS, (b) control block diagram of the VCM-FTS for thin-walled cylinder cutting

3. Simulation of thin-walled cylinder deformation

To get the empirical unit deformation function $f(z,l)$, a series of simulations are conducted. By controlling variables, three sets of simulations were used to explore the effects of force frequency, magnitude and applied point on the deformation of thin-walled cylinders.

In this study ABAQUS is chosen as a computing platform. A 3D shell model is constructed, the diameter of the shell is 60 mm, the length is 30 mm, and the thickness is 0.5 mm. One end of the shell is fixed, and a force is applied vertically to the shell surface. To explore the effects of force frequency, magnitude and applied point on the deformation, three sets of simulations are conducted. Some simulation is shown in Fig. 4.

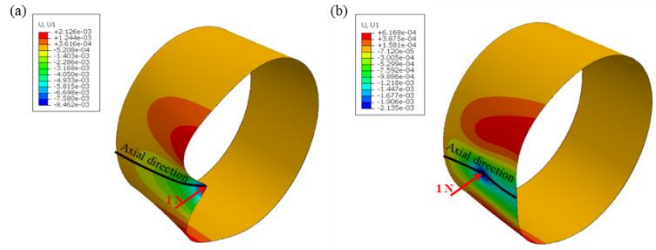

Fig. 4. axial deformation simulation of thin-walled cylindrical shell (a) force at cylinder end, (b) force at cylinder middle

Firstly, to study the effect of force frequency on thin-walled cylinder deformation, forces with different frequencies are applied to the shell. From Fig. 5(a,b), it can be found that, the difference between these 6 deformation curves is very small. Therefore, it can be concluded that if the frequency of the force is lower than 100 Hz, the effect of force frequency on thin-walled cylinder deformation is negligible.

Secondly, to investigate the effect of force magnitude, a series of simulations are conducted, each model has a different force magnitude. As shown in Fig. 5(c), the maximum deformation increases with the force magnitude. Divide the deformation by the force, and the unit force deformation curve can be obtained. From Fig. 5(d), it can be concluded that, the deformation of the thin-walled cylinder is proportional to the magnitude of the force, which means if the unit deformation u^* and the force constant k can be obtained, the true deformation can be calculated.

Finally, the influence of force applied point on thin-walled cylinder deformation is studied. If the force is applied at the region between two ends, the deformation simulation result is shown in Fig. 4(b). In this case, only the deformation from the force point to the fixed point is considered. Fig. 5(e) shows 5 different deformation curves, with the position of the force applied point ranging from 30 mm to 6 mm. It can be found that the unit deformation u^* at one point z is related to the force applied point l, namely $u^* = f(z,l)$. To obtain the unit deformation function $f(z,l)$, more simulations are conducted, and the biharmonic interpolation surface fitting method is adopted. Fig. 5(f) shows the deformation fitting surface. Although the analytical solution of $f(z,l)$ cannot be obtained, based on the fitting results, the Simulink lookup table block can be created. The function of this block is to output the unit deformation u^* when the force applied point l and axial distance z are input. Since Simulink is adopted to control the VCM-FTS in this research, this lookup table block can be directly used in the control program.

Through simulation it is found that, the influence of force frequency on thin-walled cylinder deformation is negligible; the deformation is proportional to the force magnitude; and the relation between force applied point and deformation $f(z,l)$ can be fitted into a Simulink lookup table block. Combining these results with the deformation estimation and compensation algorithm introduced in section 2.1, the deformation of the thin-walled cylinder can be estimated and compensated in real time during the cutting process.

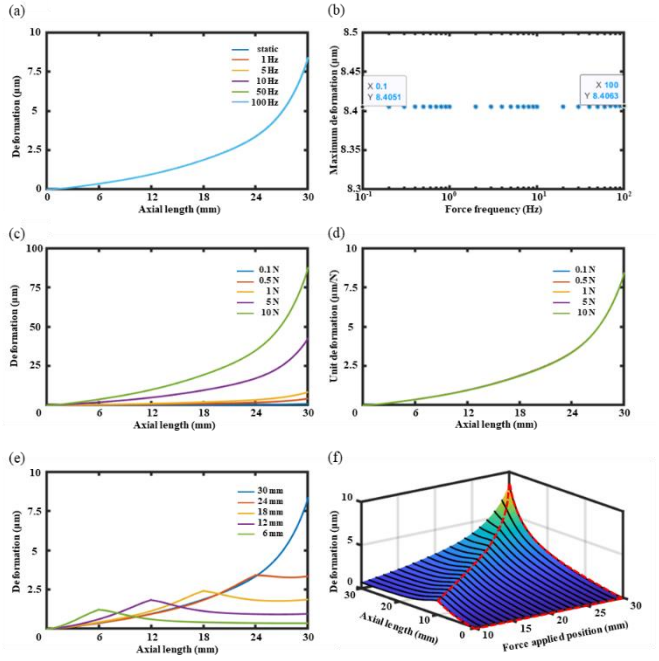

Fig. 5. Simulation results of different deformation curves for thin-walled cylinder, (a) different force frequencies, (b) enlarged view of (a), (c) different force magnitudes, (d) unit force deformation curve, (e) different force applied positions, (f) fitting surface for varying application points.

4. Cutting experiment

4.1 Experiment setup

To verify the deformation estimation and compensation method of the thin-walled cylinder in ultra-precision cutting, experimental devices are built on a three-axis ultra-precision diamond turning machine tool, as shown in Fig. 6. To prevent the workpiece from deforming during clamping, the cylinder workpiece is half solid and the half thin-walled. The outer diameter of the cylinder is 60 mm, the thickness of the shell is 0.5mm, and the lengths of the solid and thin-walled parts are 40 mm and 30mm respectively. The cylinder workpiece is first fixed on the clamp through the solid part and then mounted on the C-axis through a vacuum chuck. The measurement system consisting of three capacitive displacement sensors is installed on the machine, to measure the displacement of the workpiece. The sensor on the most left is placed next to the solid cylinder to measure the solid part displacement, and the other two sensors are used to measure the thin-walled part displacement of the workpiece. The VCM-FTS is mounted on the Z-axis of the machine via a plastic plate. The VCM-FTS is actuated by a linear amplifier. The personal computer (PC) is used as the real-time controller. To guarantee the real-time

performance of the PC controller, the Desktop real-time app in the Matlab® Simulink software is used in the control. The PC receives and outputs signals through the DAQ.

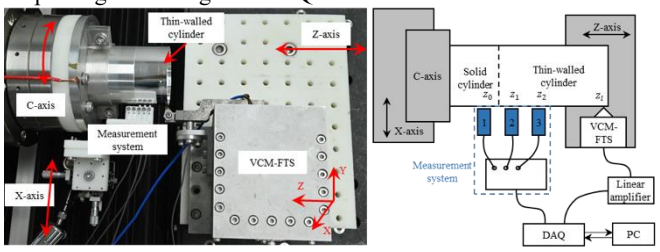

Fig. 6. Thin-walled cylinder deformation estimation and compensation cutting experimental setup.

4.2 Ultra-precision cutting experiments of double sinusoidal microstructure

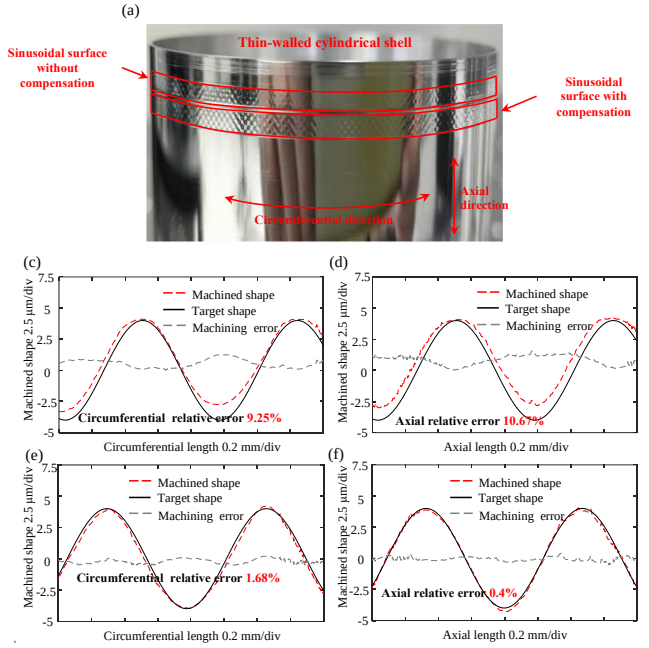

Fig. 7. Cutting results of double sinusoidal structure on thin-walled, (a) photo of double sinusoidal structure, (b) cutting error (no compensation, circumferential), (b) cutting error (no compensation, axial), (d) cutting error (with compensation, circumferential), (3) cutting error (with compensation, axial).

To explore the capability of the deformation compensation method in processing microstructures on the surface of thin-walled cylinders, double sinusoidal structures with 0.3π μm axial and circumferential period, and 4 μm sinusoidal amplitude are machined on the surface of thin-walled cylinder. Experiments with and without deformation compensation were conducted, the results are shown in Fig. 7. Without deformation, the amplitude of the circumferential surface profile of the machined workpiece is 3.63 μm, the topography error is 0.37 μm, the axial surface profile amplitude is fitted to 3.573 μm, the topography error is 0.427 μm. It can also be found that the greater the cutting depth, the larger the form error will be. In the contrast, with the deformation compensation method, the circumferential surface profile amplitude of the double sinusoidal surface is 4.067 μm, the topography error is 0.067 μm, reduced by 81.89%. The axial surface profile amplitude is 3.984 μm, the topography error is 0.016 μm, reduced by 96.25%. It can be concluded that the radial deformation caused by cutting force during processing is compensated, and the dimensional accuracy is highly improved.

5. Conclusions

In order to process microstructure arrays with high dimensional accuracy on the surface of the thin-walled cylinder, this paper proposed a deformation estimation and compensation method. With the FEM simulation, the relation between cutting force and deformation of the thin-walled cylinder was figured out, and based on that the deformation estimation method was developed. Thereafter, the controller can control the FTS and output a certain amount of displacement based on the original displacement to compensate for the deformation of the thin-walled cylinder during processing. When machining the double sinusoidal microstructure, the circumferential morphology error and axial morphology error of the microstructure were reduced by 81.89% and 96.25% respectively.

REFERENCES

1. Wang T, Zha J, Jia Q, Chen Y., “Application of low-melting alloy in the fixture for machining aeronautical thin-walled component,” Int J Adv Manuf Technol, Vol.87, pp. 2797–2807, 2016.
2. Guo J, Lee K-M, Yu M, Ma H, Xiong Z., “Regenerative Effects of Orthogonal Chip Dimensions on Turning Stability of Thin-Wall Workpiece-Tool Coupled Dynamics,” IEEEASME Trans Mechatron, Vol. 27, pp. 3601–3612, 2022.
3. Bergs T, Knappe D, Husseini K, Pullen T, Schraknepper D, Döring J-E., “Investigation of the diameter error when turning thin walled workpieces,” Procedia CIRP, Vol. 102, pp. 343–348, 2021.
4. Aijun T, Zhanqiang L, “Deformations of thin-walled plate due to static end milling force,” J Mater Process Technol, Vol. 206, pp. 345–351, 2008.
5. Manikandan H, Chandra Bera T., “Modelling of dimensional and geometric error prediction in turning of thin-walled components,” Precis Eng, Vol. 72, pp. 382–396, 2021.
6. Wan M, Zhang WH, Qin GH, Wang ZP., “Strategies for error prediction and error control in peripheral milling of thin-walled workpiece,” Int J Mach Tools Manuf, Vol. 48, pp. 1366–1374, 2008.
7. Zhu L, Li Z, Fang F, Huang S, Zhang X., “Review on fast tool servo machining of optical freeform surfaces,” Int J Adv Manuf Technol, Vol. 95, pp. 2071–2092, 2018.
8. Stöbener D, Beekhuis B., “Application of an in situ measuring system for the compensation of wall thickness variations during turning of thin-walled rings,” CIRP Annls. Vol.62, pp. 511–514, 2013.